

# Laser frequency stabilization and control through offset sideband locking to optical cavities

J. I. Thorpe<sup>1</sup>, K. Numata<sup>1,2</sup>, and J. Livas<sup>1</sup>

<sup>1</sup>NASA Goddard Space Flight Center,  
Greenbelt, MD., 20771

<sup>2</sup>Department of Astronomy, University of Maryland,  
College Park, MD., 20742

[James.I.Thorpe@nasa.gov](mailto:James.I.Thorpe@nasa.gov)

**Abstract:** We describe a class of techniques whereby a laser frequency can be stabilized to a fixed optical cavity resonance with an adjustable offset, providing a wide tuning range for the central frequency. These techniques require only minor modifications to the standard Pound-Drever-Hall locking techniques and have the advantage of not altering the intrinsic stability of the frequency reference. We discuss the expected performance and limitations of these techniques and present a laboratory investigation in which both the sideband techniques and the standard, non-tunable Pound-Drever-Hall technique reached the  $100\text{ Hz}/\sqrt{\text{Hz}}$  level.

**OCIS codes:** (140.3425) Laser Stabilization, (120.2230) Fabry-Perot

---

## References and links

1. R. Drever, J. Hall, F. Kowalski, J. Hough, G. Ford, A. Munley, and H. Ward, "Laser phase and frequency stabilization using an optical resonator," *Appl. Phys. B* **31**, 97–105 (1983).
2. J. Hall, L. Ma, M. Taubman, B. Tiemann, F. Hong, O. Pfister, and J. Ye, "Stabilization and frequency measurement of the  $I_2$ -stabilized Nd:YAG laser," *IEEE Trans. Instrum. Meas.* **48**, 583–586 (1999).
3. L. Conti, M. D. Rosa, and F. Marin, "High-spectral-purity laser system for the Auriga detector optical readout," *JOSA B* **20**, 462–468 (2003).
4. H. Zhen, H. Ye, X. Liu, D. Zhu, H. Li, Y. Lu, and Q. Wang, "Widely tunable reflection-type Fabry-Perot interferometer based on relaxor ferroelectric poly(vinylidene fluoride-chlorotrifluoroethylene-trifluoroethylene)," *Opt. Express*, **16**, 9595–9600 (2008).
5. F. Bondu, P. Fritschel, C. Man, and A. Brillet, "Ultra-high-spectral-purity laser for the Virgo experiment," *Opt. Lett.* **21**, 582–584 (1996).
6. J. Ye and J. Hall, "Optical phase locking in the microradian domain: potential applications to NASA spaceborne optical measurements," *Opt. Lett.* **24**, 1838–1840 (1999).
7. R. Pound, "Electronic frequency stabilization of microwave oscillators," *Rev. Sci. Instrum.* **17**, 490–505 (1946).
8. E. Black, "An introduction to Pound-Drever-Hall laser frequency stabilization," *Am. J. Phys.* **69**, 79–87 (2001).
9. K. Numata, A. Kemery, and J. Camp, "Thermal-noise limit in the frequency stabilization of lasers with rigid cavities," *Phys. Rev. Lett.* **93** (2004).
10. J. Alins, A. Matveev, N. Kolachevsky, Th. Udem, and T.W. Hänsch, "Subhertz linewidth diode lasers by stabilization to vibrationally and thermally compensated ultralow-expansion glass Fabry-Pérot cavities," *Phys. Rev. A* **77**, 053809 (2008).
11. S. A. Webster, M. Oxborrow, S. Pugla, J. Millo, and P. Gill, "Thermal-noise-limited optical cavity," *Phys. Rev. A* **77**, 033847 (2008).
12. B. Sheard, M. Gray, D. McClelland, and D. Shaddock, "Laser frequency stabilization by locking to a LISA arm," *Phys. Lett. A* **320**, 9–21 (2003).
13. P. Bender, K. Danzmann, and the LISA Study Team, "Laser interferometer space antenna for the detection of gravitational waves, pre-Phase A report," *Tech. Rep. MPQ233*, Max-Planck-Institut für Quantenoptik, Garching (1998). 2nd ed.

14. P. Welch, "The use of fast fourier transform for the estimation of power spectra: A method based on time averaging over short, modified periodograms," *IEEE Trans. Audio Electroacoust.* **AU-15**, 70–73 (1967).
  15. M. Tröbs and G. Heinzel, "Improved spectrum estimation from digitized time series on a logarithmic frequency axis," *Measurement* **39**, 120–129 (2005).
- 

## 1. Introduction

The linewidth, which describes deviations of the electric field's frequency from the nominal frequency  $\nu_0$ , is one of the key figures of merit for a light source. In applications such as interferometry and spectroscopy, the linewidth limits the precision of the overall measurement. Various techniques are employed to reduce the linewidth of laser sources[1, 2]. Each of these techniques requires a frequency reference with an inherent stability that exceeds that of the free-running laser.

One common such reference is an external, gain-free optical cavity constructed from dimensionally-stable materials. The length stability of the cavity can be transferred to frequency stability in the laser by tuning the laser frequency such that the round trip optical path length in the cavity is equal to an integer number of wavelengths.

A disadvantage of optical cavities as frequency references is that the central frequency can only be stabilized at a series of fixed points in frequency space separated by the *Free Spectral Range* (FSR), which for a linear two-mirror cavity is given by

$$FSR \equiv \frac{c}{2L}, \quad (1)$$

where  $c$  is the speed of light and  $L$  is the cavity length. For certain applications, such as generating an interference between two independent laser beams or probing spectroscopic features, it is advantageous to be able to adjust  $\nu_0$  with a resolution better than one FSR while still suppressing the free-running frequency noise.

There are several approaches to producing a frequency-stabilized light source with a tunable central frequency. One approach is to adjust the cavity resonance frequency by changing the length of the cavity (e.g. with a piezoelectric element as done by Conti, et. al[3]) or its optical index[4]. The disadvantage of this approach is that tunable elements in the cavity spacer will likely worsen the length stability of the cavity when compared with a fixed reference.

A second approach to a frequency-stabilized tunable light source is to lock a laser to a fixed cavity and then add an additional frequency actuator in the application beam. A commonly-used actuator is an acousto-optic frequency modulator. While AOMs have been successfully used in this application (by Bondu, et. al[5] for example), they have some drawbacks. These include relatively low bandwidth (few 100MHz) and large RF power consumption. The latter is of particular concern in power-critical applications such as space flight. AOMs also produce a frequency-dependent deflection of the beam which can be mitigated by double-passing with a curved mirror but often increases pointing noise.

Another frequency actuator that is sometimes used is an offset phase-locked slave laser (see Ye and Hall[6] for example). This produces a very quiet and flexible actuator but requires an additional laser, adding to cost and power consumption.

In this paper we propose a new approach to a tunable frequency-stabilized light source. A laser is locked to the resonance of a fixed-length cavity with a continually tunable offset frequency. The offset is generated using the phase modulator, a component which is already necessary for implementing standard frequency modulation locking techniques. The new technique retains the fundamental stability of the cavity and also requires no additional components, making it attractive for applications where simplicity and power consumption are critical.

The paper is organized as follows. In section 2, we briefly review the standard cavity locking technique. In section 3 we describe three modified techniques with tunable frequency offsets.

Section 4 delves deeper into the expected performance of the new techniques and compares with existing standard methods. Section 5 presents a laboratory demonstration of the new techniques.

## 2. Standard Pound-Drever-Hall (PDH) locking

In order to utilize an optical cavity as a frequency reference, one must generate an error signal that is proportional to the difference in frequency between the laser light and the cavity resonance. A good way to do this is to examine the light reflected from the cavity, the spectrum of which is the product of the incoming spectrum and the cavity's complex amplitude reflection coefficient,  $F(\omega)$ , where  $\omega \equiv 2\pi\nu$ . The amplitude of  $F(\omega)$  goes to zero at the resonance frequencies ( $\omega_n \equiv 2\pi n \cdot FSR$   $n = 1, 2, 3, \dots$ ) and approaches unity between them. The width of the resonance is characterized by the Finesse,  $\mathcal{F}$ , defined as

$$\mathcal{F} = \frac{FSR}{\nu_{FWHM}}, \quad (2)$$

where  $\nu_{FWHM}$  is the full width at half minimum of  $|F(\omega)|$ . It is the phase of  $F(\omega)$  that contains the information about whether the light frequency is above or below the resonance. The phase of  $F(\omega)$  begins at  $-\pi$  rad far below resonance, increases monotonically to  $-\pi/2$  rad just below resonance, goes through a discontinuity of  $\pi$  rad at resonance, and increases monotonically from  $\pi/2$  rad to  $\pi$  rad far above resonance. A measurement of the phase shift experienced by the reflected light can be used to generate an error signal for locking to the cavity resonance.

The standard technique for locking a laser to a resonance such as that formed by a cavity is Pound-Drever-Hall (PDH) [1, 7] locking. In PDH locking, the light incident on the cavity is first phase-modulated, so that the electric field is of the form

$$\tilde{E} = \sqrt{P_0} \exp\{i[\omega_c t + \beta \sin(\Omega t)]\}, \quad (3)$$

where  $P_0$  is the power incident on the modulator,  $\omega_c$  is the angular frequency of the incoming light,  $\beta$  is the modulation depth, and  $\Omega$  is the angular frequency of the modulation. To first order in  $\beta$ , the effect of phase modulation is to split the beam into three distinct frequency components: a carrier at  $\omega = \omega_c$  and two sidebands at  $\omega = \omega_c \pm \Omega$ . For sufficiently large  $\Omega$ , the sidebands are completely reflected when the carrier is near resonance, as shown in Fig. 1(a).

If the carrier is not perfectly in resonance, a portion of it will reflect and generate an intensity modulation in the reflected light by interfering with the reflected sidebands. It can be shown[8] that the reflected light power with angular frequency  $\Omega$  is given to first order in the modulation depth,  $\beta$ , by

$$\begin{aligned} P_{ref,\Omega} &= 2P_0 J_0(\beta) J_1(\beta) \text{Re}[F(\omega_c) F^*(\omega_c + \Omega) - F^*(\omega_c) F(\omega_c - \Omega)] \cos(\Omega t) \\ &+ 2P_0 J_0(\beta) J_1(\beta) \text{Im}[F(\omega_c) F^*(\omega_c + \Omega) - F^*(\omega_c) F(\omega_c - \Omega)] \sin(\Omega t), \end{aligned} \quad (4)$$

where  $J_n(x)$  is the  $n^{\text{th}}$ -order Bessel function of the first kind. When the carrier is near resonance, the bracketed term in (4) is purely imaginary and proportional to  $\delta\nu$ , the frequency offset between the carrier and the cavity resonance. The proportionality constant is known as the frequency discriminant, which for a lossless cavity is given by

$$D_{PDH} = -\frac{16\mathcal{F}LP_0}{c} J_0(\beta) J_1(\beta). \quad (5)$$

An error signal suitable for locking to the cavity resonance can be generated by measuring  $P_{ref,\Omega}$  using a photoreceiver and demodulating the output to recover the  $\sin(\Omega t)$  component.

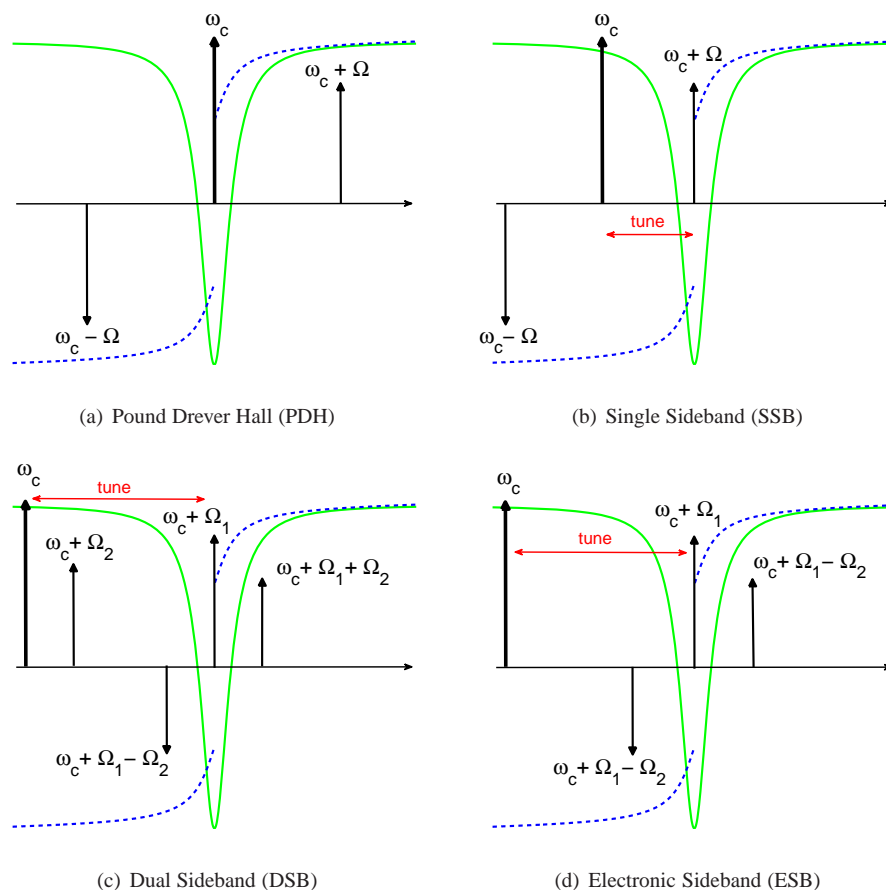


Fig. 1. Modulation structures for traditional and tunable modulation/demodulation locking. For DSB and ESB only the upper half ( $\omega \geq \omega_c$ ) of the modulation structure is shown. The solid curve represents  $|F(\omega)|^2$  and the dashed curve represents  $\angle F(\omega)$ , where  $F(\omega)$  is the amplitude reflection coefficient of the cavity. For the frequency-tunable cases, the arrow labeled *tune* indicates the frequency spacing that is adjusted to tune the carrier, denoted by a thick line.

### 3. Sideband locking

The goal of this work was to modify the standard PDH technique to allow the carrier frequency to be tunable with respect to the cavity resonances. We developed three different modulation/demodulation schemes to achieve this: single sideband locking (SSB), dual sideband locking (DSB), and electronic sideband locking (ESB). In each of these techniques, phase modulation is used to generate a sideband which is locked to the cavity resonance. The frequency of the carrier is then adjusted by changing the frequency used to generate the sideband. In practice, a portion of the source beam is picked off and used to perform the frequency stabilization. The remaining light, free of any modulation sidebands, tracks the carrier frequency.

### 3.1. Single Sideband (SSB) locking

The single sideband locking (SSB) technique is the simplest modification to the standard PDH technique that provides tunability. The same modulation scheme is used, but with the modulation frequency  $\Omega$  being adjustable and with one of the sidebands locked to the resonance rather than the carrier (See Fig. 1(b)). The expression for  $P_{ref,\Omega}$  in (4) is still valid only one of the sidebands is resonant while the other sideband and the carrier are reflected. If we redefine the resonance frequencies as  $\omega_n \equiv 2\pi n \cdot FSR + (-)\Omega$  for locking on the upper(lower) sideband, the  $\sin(\Omega t)$  component is proportional to  $\delta v$  with a discriminant given by

$$D_{SSB} = \frac{8\mathcal{F}LP_0}{c} J_1(\beta) [J_0(\beta) - J_2(\beta)]. \quad (6)$$

The  $J_2(\beta)$  term arises from interference between the resonant sideband and a second sideband at  $\omega_c \pm 2\Omega$  that appears when the expansion of (3) is taken to higher orders in  $\beta$ . For small  $\beta$ ,  $D_{SSB}$  is of opposite sign and a factor of two lower than  $D_{PDH}$ . Once one of the sidebands is locked to the cavity resonance, the carrier frequency can be tuned by adjusting  $\Omega$ .

### 3.2. Dual Sideband (DSB) locking

The dual sideband (DSB) technique uses a modulation spectrum that is identical to that used for PDH locking with a tunable offset from the carrier. This can be accomplished by modulating the beam at two distinct frequencies, one of which is adjustable. Consider a light beam with power  $P_0$  and angular frequency  $\omega_c$  that is phase-modulated with two sinusoidal signals of depth  $\beta_i$  and angular frequency  $\Omega_i$  ( $i = 1, 2$ ). The electric field is given by,

$$\tilde{E}_{DSB} = \sqrt{P_0} \exp \{i[\omega_c t + \beta_1 \sin(\Omega_1 t) + \beta_2 \sin(\Omega_2 t)]\}. \quad (7)$$

Expanding to first order in  $\beta_{1,2}$ , the result of the phase modulation is a carrier with angular frequency  $\omega_c$ , sidebands with angular frequencies  $\omega_c \pm \Omega_1$ , sidebands with angular frequencies  $\omega_c \pm \Omega_2$ , and sub-sidebands at  $\omega_c + \Omega_1 \pm \Omega_2$  and  $\omega_c - \Omega_1 \pm \Omega_2$ .

The modulated spectrum for  $\omega \geq \omega_c$  is shown in Fig. 1(c) assuming  $\Omega_1 > \Omega_2$  and  $\beta_1 > \beta_2$ . Note that the spectral structure centered around  $\omega_c + \Omega_1$  with sidebands offset by  $\pm\Omega_2$  is analogous to the PDH modulation spectrum in Fig. 1(a). In DSB locking, this structure (or the analogous one at  $\omega_c - \Omega_1$ ) is used to generate an error signal by placing one of the  $\omega_c \pm \Omega_1$  sidebands on resonance and demodulating the reflected power with  $\Omega_2$ . The frequency discriminant is given by

$$D_{DSB} = \frac{16\mathcal{F}LP_0}{c} J_1^2(\beta_1) J_0(\beta_2) J_1(\beta_2). \quad (8)$$

Frequency tuning of the carrier can be accomplished by adjusting  $\Omega_1$ .

One disadvantage of the DSB technique is that the complex modulation structure leads to the generation of spurious error signals. This can make lock acquisition challenging and also provides potential pathways for noise to enter the system. In particular, a PDH error signal will be generated when the carrier is in resonance and the power is demodulated by  $\Omega_2$ . If the modulation depth of the first modulator is not large enough to sufficiently suppress the carrier, this error signal may even be larger than the desired DSB error signal. The situation becomes even more complex when additional resonances due to higher-order cavity spatial modes are present.

### 3.3. Electronic Sideband (ESB) locking

The electronic sideband (ESB) technique simplifies the modulated spectrum of the DSB technique by eliminating the  $\omega_c \pm \Omega_2$  sidebands. This can be accomplished by driving a single

broadband phase-modulator with a phase-modulated drive signal. The drive signal has a carrier frequency of  $\Omega_1$  and is phase-modulated at  $\Omega_2$  with a depth of  $\beta_2$ . This signal is then used to drive the phase modulator with a depth of  $\beta_1$ . The electric field of the light exiting the modulator is of the form

$$\tilde{E}_{ESB} = \sqrt{P_0} \exp\{i[\omega_c t + \beta_1 \sin(\Omega_1 t + \beta_2 \sin \Omega_2 t)]\}. \quad (9)$$

Expanding to first order in  $\beta_i$ , the spectrum is identical to the DSB structure with the exception that the  $\omega_c \pm \Omega_2$  sidebands are removed. Figure 1(d) shows this spectrum for  $\omega \geq \omega_c$ . The error signal is generated by placing one of the  $\omega_c \pm \Omega_1$  sidebands near resonance and demodulating with  $\Omega_2$ . As with DSB, the carrier is tuned by adjusting  $\Omega_1$ .

The power in the  $\omega_c \pm \Omega_1$  sidebands and the  $\omega_c \pm \Omega_1 \pm \Omega_2$  sub-sidebands is the same as for the DSB case. As a result, the frequency discriminant for ESB locking is identical to that given in (8) for DSB. The power in the carrier is increased to  $P_0 J_0^2(\beta_1)$  for ESB versus  $P_0 J_0^2(\beta_1) J_0^2(\beta_2)$  for DSB.

#### 4. Technique comparison

The preceding sections defined four locking schemes (PDH, SSB, DSB, and ESB) and derived their frequency discriminants. In this section we attempt to compare the relative merits of the four techniques in terms of noise performance, tuning, and implementation.

##### 4.1. Fundamental noise limits

The ultimate frequency noise limit of cavity-stabilized lasers is set by two effects: shot noise and cavity thermal noise. Shot noise generates white optical power noise at the photoreceiver with a level of

$$S_{shot,P} = \sqrt{\frac{2hc}{\lambda} P_{ref}}, \quad (10)$$

where  $h$  is Planck's constant,  $\lambda$  is the vacuum wavelength of the light, and  $P_{ref}$  is the reflected light power on resonance. For a perfectly coupled cavity,  $P_{ref}$  will be equal to  $P_0$ , the total power incident on the modulator(s), less the power of the resonant spectral component.

The frequency noise associated with shot noise can be estimated[8] by dividing  $S_{shot,P}$  by the frequency discriminant,  $D$ . Table 1 lists  $P_{ref}$ ,  $D$ ,  $\beta_{opt}$ , the optimal modulation depth for shot noise limited operation, and  $S_{shot,v}$ , the shot-noise limited frequency noise floor for  $\beta = \beta_{opt}$ . The shot noise floors for the sideband systems in table 1 are five to six times larger than the floor for the traditional PDH system,

$$\begin{aligned} (S_{shot,v})_{PDH} &= \frac{1}{8L\mathcal{F}} \sqrt{\frac{hc^3}{P_0\lambda}} \\ &= \left(277 \mu\text{Hz}/\sqrt{\text{Hz}}\right) \left(\frac{20\text{cm}}{L}\right) \left(\frac{10^4}{\mathcal{F}}\right) \left(\frac{1\mu\text{m}}{\lambda}\right)^{1/2} \left(\frac{1\text{mW}}{P_0}\right)^{1/2}. \end{aligned} \quad (11)$$

Cavity thermal noise refers to Brownian motion of the various cavity components. Numata, et. al[9] estimated the thermal noise floor for a room-temperature optical cavity with an ultra-stable glass spacer and dielectric-coated mirrors to be roughly  $\sim 50\text{mHz}/\sqrt{\text{Hz}} \cdot \sqrt{1\text{Hz}/f}$ .

Comparing this level with the shot noise limit demonstrates that for a cavity with the parameters specified in (11), the shot noise of the tunable sideband techniques will be below the thermal noise limit for Fourier frequencies below  $\sim 500\text{Hz}$ . In these cases, no penalty in fundamental noise is paid by using the sideband technique as compared to the traditional PDH technique.

Table 1. Shot noise limited frequency noise for each locking technique at optimum modulation depth, assuming perfect contrast in the cavity resonance.

Technique	$P_{ref}/P_0$	$ D  \times \left(\frac{\mathcal{F}LP_0}{c}\right)^{-1}$	$\beta_{opt}$	$S_{shot,v} / (S_{shot,v})_{PDH}$
PDH	$1 - J_0^2(\beta)$	$16J_0(\beta)J_1(\beta)$	$0^\dagger$	1
SSB	$1 - J_1^2(\beta)$	$8J_1(\beta)[J_0(\beta) - J_2(\beta)]$	0.97	4.4
DSB/ESB	$1 - J_1^2(\beta_1)J_0^2(\beta_2)$	$16J_1^2(\beta_1)J_0(\beta_2)J_1(\beta_2)$	$\beta_1 \rightarrow 1.84$ $\beta_2 \rightarrow 1.01$	5.5

<sup>†</sup>This is a theoretical optimum for perfect contrast and no technical noise. When the effects of finite contrast and technical noise are included, the optimum modulation depth will increase.

#### 4.2. Technical noise

Although some measurements have been shown to approach the fundamental noise limits [10, 11], in most cases the noise performance of any particular cavity system is set by a number of technical noises. Noises which affect the stability of the reference directly (e.g. temperature and vibration fluctuations in the cavity) will obviously affect all stabilization systems equally. Other noise sources will differ between the different techniques. One effect is the smaller frequency discriminants of the sideband systems, which require the addition of electronic gain in order to reach the same closed-loop gain as an equivalent PDH system. This electronic gain carries with it a noise penalty. For optimal modulation depths, the frequency discriminants of the sideband techniques are a factor of two to three smaller than an equivalent PDH system. If the noise sources of interest are suppressed by more than that factor below the fundamental noise sources, there will no noise penalty paid by adding frequency tunability through sideband locking.

A technical noise source in which the locking techniques differ more fundamentally is radio-frequency amplitude modulation (RFAM), also referred to as residual amplitude modulation. RFAM is unwanted amplitude modulation of the beam probing the cavity at the phase modulation/demodulation frequency. Since these modulations are at the demodulation frequency, they are not rejected like other high-frequency noise sources. Instead they produce offsets in the error signal which are sensitive to laser intensity, alignment, and other slowly-varying noise sources. These offsets provide a pathway for these noise sources to couple into the frequency noise of the stabilized laser.

SSB generates RFAM due to the fact that the light reflected from the cavity is lacking the one first order sideband that is resonant in the cavity. This leads to a strong amplitude modulation. From (4), the  $\cos(\Omega t)$  component in  $P_{ref,\Omega}$  does not vanish but instead remains with a magnitude of  $2P_0J_0(\beta)J_1(\beta)$ . Since this offset appears in the opposite quadrature as the error signal, it does not couple completely but is instead reduced by a factor of  $\approx 1 - \delta\theta^2$ , where  $\delta\theta$  is the error in the demodulation phase. DSB and ESB locking retain the symmetry of PDH locking and avoid this effect. There will, however, be certain values of the modulation frequencies, for example  $\Omega_1 = 2\Omega_2$  for DSB, where interference between the sidebands and sub-sidebands can generate RFAM at the demodulation frequency. This type of interference can be mitigated by maintaining  $\Omega_1 \gg \Omega_2$ .

Real EOMs produce some level of RFAM along with their phase modulation. This is in part due to their finite modulation bandwidth and non-zero passband ripple which cause asymmetries in the amplitudes of the phase modulation sidebands. This is of greatest concern for ESB locking, where the relevant sidebands (the  $\pm\Omega_1 \pm \Omega_2$  sub-sidebands) are introduced onto the light at higher frequencies than for DSB or PDH locking. To first order in  $\beta_2$ , passband ripple

will lead to RFAM with an amplitude of

$$AM_{ESB} \sim 2P_0\Omega_2 G'(\Omega_1) J_1(\beta_2) J_0^2(\beta_1), \quad (12)$$

where  $G'(\Omega_1)$  is the derivative with respect to modulation frequency of the modulator response around the frequency  $\Omega_1$ . The amplitude can be reduced by reducing the modulation frequency,  $\Omega_2$  or, if necessary, measuring the modulator response and constructing a compensation filter for the RF drive that will reduce  $G'(\Omega_1)$ .

Lastly, RFAM can arise through various imperfections in the phase modulators themselves or through beam pointing modulations introduced by the EOM which cause the beam to wander over regions of varying sensitivity on the reflected light photoreceiver. These mechanisms affect all four techniques at roughly the same level.

#### 4.3. Tuning range and bandwidth

For the frequency tunable systems, the tuning dynamic range and slew-rate are important figures of merit. The range of offsets from the cavity resonance that can be achieved through slow adiabatic tuning is limited primarily by the RF components used for modulation / demodulation. For each of the techniques, the tuning range will be limited by the bandwidth of the EOM and the associated drive electronics. For typical bulk crystal EOMs, bandwidths of  $\sim 100$  MHz are readily available, although the amount of RF power needed to drive these broadband EOMs to sufficient modulation depths is large. Waveguide modulators can deliver high modulation depths over bandwidths exceeding 10 GHz with low drive powers, making them an attractive option for this application.

In the SSB case, the demodulation frequency varies and as a result the photoreceiver and mixer bandwidths also limit the tuning range. Since the demodulation frequency remains fixed for DSB and ESB, the bandwidth requirements on the demodulation components for these techniques are identical to those for PDH.

For systems that do not require continuous tuning, it is possible to achieve an extremely large tuning range through a combination of selecting different cavity resonances and offset sideband locking. A tuning bandwidth of 1-2 FSR would be sufficient for this approach. In this case the net tuning range would be limited only by the tuning range of the laser itself.

The maximum slew-rate of the frequency tuning will be limited by the ability of the stabilization servo to track the requested frequency changes. In terms of bandwidth, it is not uncommon for PDH systems to have unity-gain bandwidths of  $\sim 100$  kHz. A large tuning bandwidth is essential if the offset sideband systems are to be used as pre-stabilization stages in a multi-stage frequency stabilization loop, such as arm-locking[12] in the Laser Interferometer Space Antenna[13].

## 5. Laboratory demonstration

The previous section described the concept of the frequency-tunable sideband locking techniques and explored some of the expected differences between each of the techniques and the standard PDH technique. In this section we present a laboratory investigation of the noise performance of each of the techniques. To focus on the differences between the techniques, a cavity system was constructed which could be re-configured to implement each of the four techniques (PDH, SSB, DSB and ESB) simply by changing the electrical signals fed to the modulators and demodulation electronics. The goal was to demonstrate significant noise suppression over the free-running laser noise while investigating the effects of adding tunable center frequencies.

### 5.1. Experimental configuration

The multi-technique optical cavity system, referred to as the test system, is shown in Fig. 2. The cavity consists of two fused-silica mirrors optically contacted to a spacer of ultra-low expansion (ULE) glass. It is housed in a vacuum tank and surrounded by a nested set of five gold-coated stainless-steel cylinders with Macor spacers to provide passive thermal shielding. The laser output first passes through a broad-band (bandwidth  $\approx 100$  MHz) bulk crystal EOM followed by a resonant bulk crystal EOM. The light transmits through a polarizing beam splitter (PBS), passes through a quarter wave-plate and reflects off of the front mirror of the cavity. The light reflected from the cavity reflects at the PBS and is collected at the photoreceiver. The photoreceiver output is demodulated using an analog mixer and the mixer output is filtered and fed into the frequency-tuning ports on the laser. The laser can be locked to the cavity using any of the four locking techniques: standard PDH locking, SSB locking, DSB locking, or ESB locking. Table 2 lists the signals that are connected to the EOMs and the mixer in order to realize each technique.

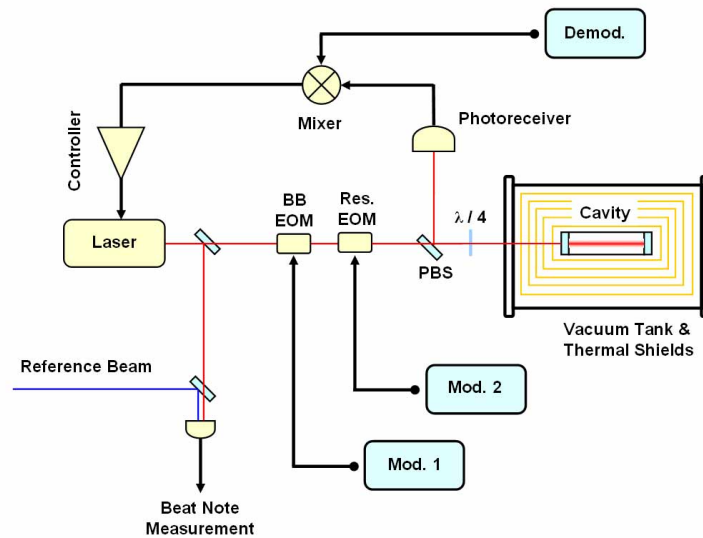


Fig. 2. Arrangement of test cavity systems for experiments described in section 5. Table 2 lists the modulation/demodulation signals used for each locking technique. The reference beam was sourced from a laser locked to an independent cavity using the standard Pound-Drever-Hall technique.

An independent laser/cavity system is used to provide a reference for measuring the frequency stability of the test system. It is configured similarly to the test system with the exception that only a single resonant EOM is present and consequently only the PDH locking scheme is used. A portion of the output of each laser is split off before the EOMs and interfered at a beam-splitter, generating a beat note that is monitored with an wide-band photoreceiver.

### 5.2. Results & discussion

The noise performance of the PDH and SSB techniques are presented in Fig. 3. The curves plotted are estimates of  $\sqrt{S_{\Delta\nu}(f)}$ , the linear spectral density (LSD) of the frequency noise of

Table 2. Modulation/Demodulation signals used for each locking technique. See Fig. 2 for corresponding block diagram. (PDH = Pound-Drever-Hall locking, SSB = single sideband locking, DSB = dual sideband locking, ESB = electronic sideband locking)

Technique	Mod. 1	Mod. 2	Demod	Tuning
PDH	none	$\Omega$ , fixed	$\Omega$ , fixed	none
SSB	$\Omega$ , variable	none	$\Omega$ , variable	$\Omega$
DSB	$\Omega_1$ , variable	$\Omega_2$ , fixed	$\Omega_2$ , fixed	$\Omega_1$
ESB	$\Omega_1$ w/ phase mod. at $\Omega_2$	none	$\Omega_2$ , fixed	$\Omega_1$

the beat note between the test and reference systems. Two spectra are shown in Fig. 3 for the SSB case, one where the carrier frequency was held fixed and one where a reference frequency-modulation tone with amplitude 1 kHz and frequency  $\approx 900 \mu\text{Hz}$  was added to the EOM drive. The spectrum with the modulation tone was estimated using a periodograms with linear frequency bin spacing[14] while the other spectra used logarithmically-spaced bins[15] for improved amplitude estimation.

The noise spectra for the traditional PDH case and the SSB case without modulation are virtually identical, indicating that, in this particular realization, the SSB technique performs at least as well as PDH. For the case where the modulation is added, the noise floor at frequencies other than the modulation frequency is unchanged, demonstrating that the central frequency can be tuned without sacrificing broad-band frequency stability. Results similar to those in Fig. 3 were obtained with both the DSB and ESB techniques as well. Also shown for reference is the free-running noise, obtained with no stabilization, which demonstrates that the stabilization techniques reduce the noise in a given frequency band by a factor of  $10^4 - 10^5$ .

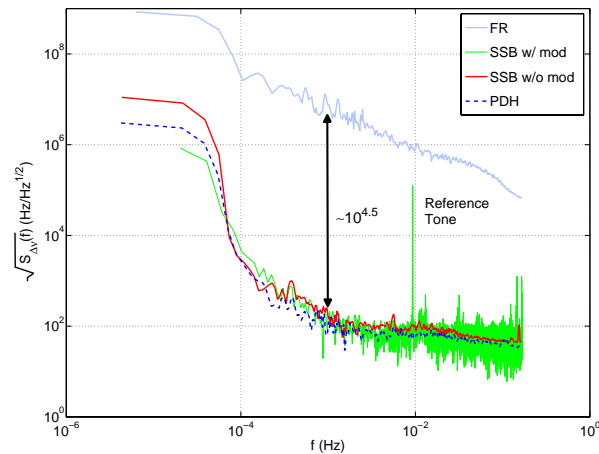


Fig. 3. Beat note frequency noise spectra for free-running lasers (FR), Pound-Drever-Hall locking (PDH), and single-sideband locking (SSB). For the “SSB w/ mod” case, a frequency modulation with 1.00 kHz amplitude at a frequency of  $\approx 900 \mu\text{Hz}$  was added to the SSB tuning port. The measured amplitude of the reference tone is 0.983 kHz after accounting for the spectrum’s equivalent noise bandwidth.

The fact that the sideband systems performed as well as the PDH system suggests that the limiting noise sources are common to each of the techniques. A noise model was developed to estimate the contribution from a number of potential sources. The model suggests that for

$f \leq 40 \mu\text{Hz}$ , the frequency noise is limited by thermal expansion of the cavities driven by variations in the room temperature. The thermal filter provided by the shields and vacuum tank surrounding the cavity result in the steep  $\sim f^{-7}$  slope of the noise floor in this frequency band. Above  $40 \mu\text{Hz}$ , the limiting noise sources are less certain. Likely possibilities include pointing noise, vibration noise, RFAM, and intensity noise coupling into cavity length changes through absorption and heating.

## 6. Conclusion

The ability to tune the central frequency of a cavity-stabilized laser while maintaining frequency stability has many potential applications. Offset sideband locking is a convenient way to realize this capability, as it requires only minor modifications to the standard PDH locking technique. These techniques have frequency discriminants that are only a factor of two to three lower in magnitude than equivalent PDH systems, assuming optimal modulation depths. The shot noise limited noise levels for the sideband systems are expected to be a factor of  $\sim 5$  worse than traditional PDH locking, which for low-frequency applications is not significant enough to increase the shot noise above cavity thermal noise. These techniques can also be applied to other frequency references that utilize the PDH locking scheme, such as spectroscopic references.

Our laboratory results indicate that the noise performance of the tunable systems are comparable to the standard PDH locking technique to the  $\sim 100 \text{Hz} \sqrt{\text{Hz}}$  level or better. This level is already sufficient for a number of applications, including pre-stabilization for the Laser Interferometer Space Antenna.

## Acknowledgments

This research was supported by an appointment to the NASA Postdoctoral Program at the Goddard Space Flight Center, administered by Oak Ridge Associated Universities through a contract with NASA.